First-Principles Quantum Chemical Study of Thermal Decomposition Routes for the Cationic Catalyst L_2TiMe^+

Tebikie Wondimagegn, Kumar Vanka, Zhitao Xu, and Tom Ziegler*

Department of Chemistry, University of Calgary, Calgary, Alberta, Canada T2N 1N4

Received July 13, 2004

Density functional theory has been used to investigate the various decomposition pathways involving the cationic catalyst systems L_2TiMe^+. The cationic catalyst systems include $(NPR_3)_2TiMe^+$, $(Cp)(NPR_3)TiMe^+$, $(Cp)(NCR_2)TiMe^+$, $(Cp)(SiMe_2NR)TiMe^+$, and $(Cp)(OSiR_3)TiMe^+$. The possible decomposition routes for the above catalyst systems include transfer of methyl on the butyl group from the ancillary ligand to the metal center, transfer of butyl from the ancillary ligand to the metal center, transfer of hydrogen of methyl on the butyl group from the ancillary ligand to the metal center, and transfer of methyl on Si (this is the case for the constrained-geometry catalyst) to the metal. The activation barriers for the above decomposition reactions fall in the range 16−63 kcal/mol. The transfer of methyl on the butyl group from the ancillary ligand to the metal center is more facile for the constrained-geometry catalyst than the other catalyst systems considered in this study. Furthermore, the transfer of butyl from the ancillary ligand to the metal center is a potential deactivation pathway for $(NPR_3)_2TiMe^+$, $(Cp)(NPR_3)TiMe^+$, $(Cp)(NCR_2)TiMe^+$, and $(Cp)(OSiR_3)TiMe^+$. However, this is not the case for $(Cp)(SiMe_2NR)TiMe^+$ systems. Ring-metalated metallacyclic complexes that result from an intramolecular C−H activation are also potential deactivation pathways for the catalyst systems considered in this study.

Introduction

The development of new single-site olefin polymerization catalysts that do not exclusively contain the bis-cyclopentadienyl (bis-Cp) ancillary ligands has experienced a phenomenal acceleration over the past few years.[1] A variety of strategies have been employed to explore the potential of other ligand systems. The most common way of developing such catalyst systems has been to replace one or both of the Cp ligands in the metallocenes by other donor groups. A notable example of this approach is the so-callled "constrained-geometry catalysts" first introduced by Bercaw[2] and now commercially used by Dow[3] and Exxon,[4] by combining Cp ligands with an amide functionality. More recently, a number of $Cp(L)TiX_2$ systems (L = OR,[5] NCR_2,[6] NR_2,[7] NPR_3,[8] SR,[9] and alkyl[10]) have been prepared and tested in olefin polymerization catalysis. Stephan et al have also developed several families of highly active Ti-containing olefin polymerization catalysts with bis-(phosphinimide) as ancillary ligands.[11] In general, in conjunction with activators such as methylaluminoxane (MAO), $B(C_6F_5)_3$, and $[A]^+[B(C_6F_5)_4]^-$ (A = CPh_3, HNR_3), the aforementioned complexes have been found to provide catalysts with moderate to high activity, making them viable alternatives to the metallocene systems.

However, these catalyst systems have also been found to undergo deactivating side reactions, leading to the eventual poisoning of the catalyst, thereby decreasing their productivity. The types of deactivation pathways are determined by the strength of the cation−anion interaction. For contact ion pairs, a number of deactivation pathways have been observed for the catalyst systems involved in borane and trimethylaluminum activations. The most commonly observed deactivation pathway is C_6F_5-group transfer to the cationic metal center.[12] We have recently reported another commonly observed deactivation pathway, which involves hydro-

* To whom correspondence should be addressed. E-mail: ziegler@ucalgary.ca.

(1) (a) Britovsek, G. P.; Gibson, V. C.; Waas, D. F. *Angew. Chem., Int. Ed.* **1999**, *38*, 429. (b) Liang, L-C.; Schrock, R. R.; Davis, W. M.; McConville, D. H. *J. Am. Chem. Soc.* **1999**, *121*, 5797. (c) Baumann, R.; Stumpf, R.; Davis, W. M.; Liang, L.-C.; Schrock, R. R. *J. Am. Chem. Soc.* **1999**, *121*, 7822. (d) Zhang, S.; Piers, W. E.; Gao, X.; Parvez, M. *J. Am. Chem. Soc.* **2000**, *122*, 5499. (e) Guerin, F.; Stewart, J. C.; Beddie, C.; Stephan, D. W. *Organometallics* **2000**, *19*, 2994.

(2) (a) Piers, W. E.; Shapiro, P. J.; Bunel, E. E.; Bercaw, J. E. *Synlett* **1990**, *1*, 74. (b) Shapiro, P. J.; Cotter, W. D.; Schaefer, W. P.; Labinger, J. A.; Bercaw, J. E. *J. Am. Chem. Soc.* **1994**, *116*, 4623.

(3) Stevens, J. C.; Timmers, F. J.; Wilson, D. R.; Schmidt, G. F.; Nickias, P. N.; Rosen, R. K.; Knight, G. W.; Lai, S. European Patent Appl. EP 416 815-A2, 1991 (Dow Chemical Corp.).

(4) Canich, J. M.; Hlatky, G. G.; Turner, H. W. PCT Appl. WO-A-00333, 1992 (Exxon Chemical Co.).

(5) (a) Vilardo, J. S.; Thorn, M. G.; Fanwick, P. E.; Rothwell, I. P. *Chem. Commun.* **1998**, 2425. (b) Thorn, M. G.; Vilardo, J. S.; Fanwick, P. E.; Rothwell, I. P. *Chem. Commun.* **1998**, 2427. (c) Sarsfield, M. J.; Ewart, S. W.; Tremblay, T. L.; Roszak, A. W.; Baird, M. C. *J. Chem. Soc., Dalton Trans.* **1997**, 3097. (d) Ewart, S. W.; Sarsfield, M. J.; Jeremic, D.; Tremblay, T. L.; Williams, E. F.; Baird, M. C. *Organometallics* **1998**, *17*, 1502.

(6) Zhang, S.; Piers, W. E.; Gao, X.; Parvez, M. *J. Am. Chem. Soc.* **2000**, *122*, 5499.

(7) (a) Bai, Y.; Roesky, H. W.; Noltmeyer, M. *Z. Anorg. Allg. Chem.* **1991**, *31*, 3887. (b) Schiffino, R. S.; Crowther, D. J. U.S. Patent No. 5,625,016, 1997 (Exxon Chemical Co.).

(8) Stephan, D. W.; Stewart, J. C.; Guerin, F.; Spence, R. E. v. H.; Xu, W.; Harrison, D. G. *Organometallics* **1999**, *18*, 1116.

(9) Klapötke, T.; Laskowski, R.; Köpf, H. *Z. Naturforsch., Teil B* **1987**, *42*, 777.

(10) (a) Ewart, S. W.; Baird, M. C. *Top. Catal.* **1999**, *7*, 1. (b) Mena, M.; Royo, P.; Serrano, R.; Pellinghelli, A.; Tiripicchio, A. *Organometallics* **1989**, *8*, 476.

(11) Stephan, D. W.; Guerin, F.; Spence, R. E. v. H.; Koch, L.; Gao, X.; Brown, S. J.; Swabey, J. W.; Wang, Q.; Xu, W.; Zoricak, P.; Harrison, D. J. *Organometallics* **1999**, *18*, 2046.

10.1021/om049478s CCC: $27.50
Publication on Web 10/20/2004

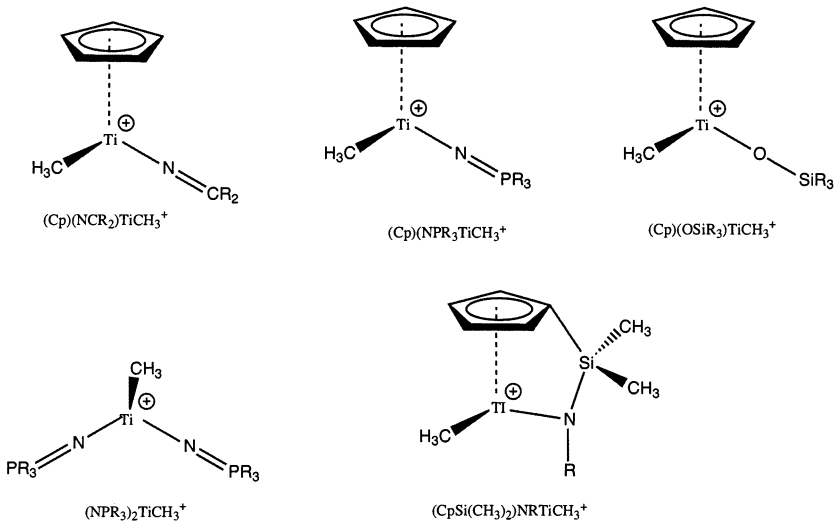

Figure 1. Structures of the cationic catalyst systems under investigation.

gen transfer from the bridging methyl group to the growing chain.[13] For weakly coordinating anions, the catalytic active species can be regarded as an essentially free cation, especially in polar solvents. In this paper, we report various deactivation pathways involving the free cationic species L_2TiMe^+.

Computational Methods and Details

Density functional theory calculations were carried out using the Amsterdam Density Functional (ADF) program system, developed by Baerends et al.[14] and vectorized by Ravenek.[15] The numerical integration scheme applied was developed by te Velde et al.,[16] and the geometry optimization procedure was based on the method of Verslius and Ziegler.[17] The electronic configurations of the atom were described by a triple-ζ basis set on titanium ($n = 3$), augmented with a single (n+1)p polarization function. Double-ζ STO basis sets were used for carbon (2s, 2p), hydrogen (1s), and nitrogen (2s, 2p), augmented with a single 3d polarization function, except for hydrogen, where a 2p polarization function was used. Shells of lower energy were treated by the frozen-core approximation. A set of auxiliary s, p, d, f, and g STO functions centered on all nuclei was used to fit the molecular density and represent Coulomb and exchange potentials accurately in each SCF cycle. All the calculations used the PW91 exchange−correlation functional.[18]

Results and Discussion

The thermal decomposition of single-site olefin polymerization catalysts at higher temperatures and pressures is of great interest for industrial scale applications. In this paper, which is the first theoretical investigation of thermal decomposition routes involving the cationic catalysts systems, we shall demonstrate how electronic effects can modulate the activation barrier and the heat of reaction. A bond order analysis[19] will be used to explain the thermodynamic stability of the product formed from the corresponding decomposition pathway. The five different cationic catalyst systems considered under this investigation are shown in Figure 1. Scheme 1 shows the different deactivation pathways involving the ketimide, siloxy, phosphinimide, and bis(phosphinimide) cationic catalyst systems. As shown in Scheme 1, the possible decomposition routes for the above catalyst systems include transfer of methyl on the butyl group from the ancillary ligand to the metal center, transfer of butyl from the ancillary ligand to the metal center, and transfer of hydrogen of methyl on the butyl group from the ancillary ligand to the metal center. The deactivation pathways for the constrained-geometry catalyst include transfer of methyl of the butyl group from the ancillary ligand to the metal center, transfer of hydrogen of methyl on the butyl group from the ancillary ligand to the metal center, and transfer of methyl on Si to the metal. These deactivation pathways are depicted in Scheme 2.

We have also considered two deactivation pathways that result from an intramolecular C−H activation to produce methane and a ring-metalated metallacyclic complex. The first reaction involves the transfer of hydrogen from the ancillary ligand to the growing polymer (CH_3). This is the case for all the catalyst systems (see Figure 1). The second deactivation pathway involves the transfer of hydrogen from C_5Me_5 (Cp*) to the growing polymer. This deactivation pathway is not applicable for the bis(phosphinimide) catalyst system, as it does not have a Cp* ring. These deactivation pathways are shown in Scheme 3.

The transition state structures were optimized for all of the decomposition routes considered in this investiga-

(12) Wondimagegn, T.; Xu, Z.; Vanka, K.; Ziegler, T. *Organometallics* **2004**, *23*, 3847.
(13) Wondimagegn, T.; Vanka, K.; Xu, Z.; Ziegler, T. *Organometallics* **2004**, *23*, 2651.
(14) (a) Baerends, E. J.; Ellis, D. E.; Ros, P. *Chem. Phys.* **1973**, *2*, 41. (b) Baerends, E. J.; Ros, P. *Chem. Phys*. **1973**, *2*, 52. (c) te Velde, G.; Baerends, E. J. *J. Comput. Phys*. **1992**, *92*, 84. (d) Fonseca, C. G.; Visser, O.; Snijders, J. G.; te Velde, G.; Baerends, E. J. In *Methods and Techniques in Computational Chemistry, METECC-95*; Clementi, E., Corongiu, G., Eds.; STEF; Cagliari, Italy, 1995; p 305.
(15) Ravenek, W. In *Algorithms and Applications on Vector and Parallel Computers*; te Riele, H. J. J., Dekker, T. J., vand de Horst, H. A., Eds.; Elservier: Amsterdam, 1987.
(16) (a) te Velde, G.; Baerends, E. J. *J. Comput. Chem.* **1992**, *99*, *84*. (b) Boerrigter, P. M.; te Velde, G.; Baerends, E. J. *Int. J. Quantum Chem.* **1998**, *33*, 87.
(17) Verslius, L.; Ziegler, T. *J. Chem. Phys*. **1988**, *88*, 322.
(18) Perdew, J. P.; Chevary, J. A.; Vosko, S. H.; Jackson, K. A.; Pederson, M. R.; Fiolhais, C. *Phys. Rev. B* **1992**, *46*, 6671.
(19) Michalak, A.; DeKock, R. L.; Ziegler, T., Manuscript in preparation. The bond order method employed in this work is a modification of that published by Nalewajski and co-workers. (a) Nalewajski, R. F.; Mrozek, J. *Int. J. Quantum Chem*. **1994**, *51*, 187. (b) Nalewajski, R. F.; Mrozek, J.; Michalak, A. *Int. J. Quantum Chem.* **1997**, *61*, 589.

Scheme 1. Cationic Decomposition Pathways Involving the Ketimide, Siloxy, Phosphinimide, and Bis(phosphinimide) Systems

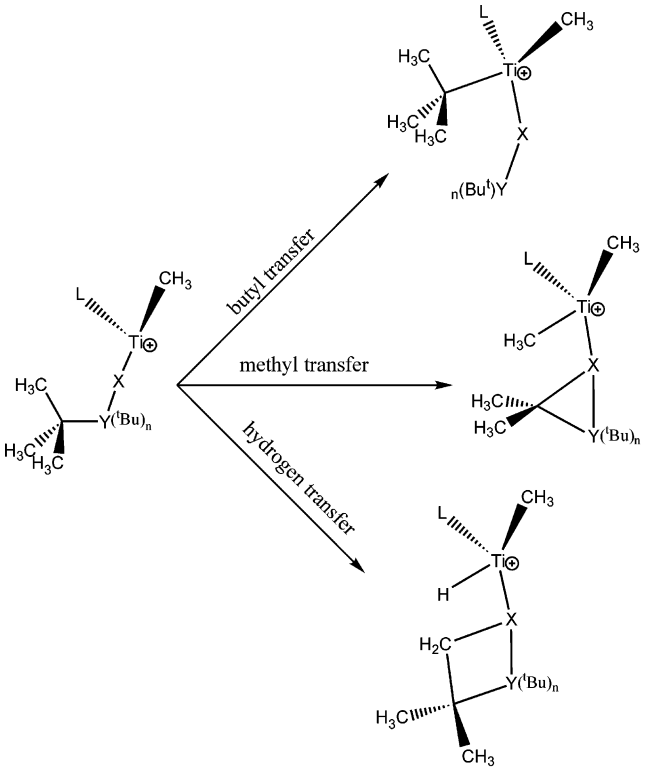

L = Cp, NP^tBu_3

X = N, O; Y = C, Si, P

n = 1, 2

Scheme 2. Cationic Decomposition Pathways Involving the Constrained-Geometry Catalyst

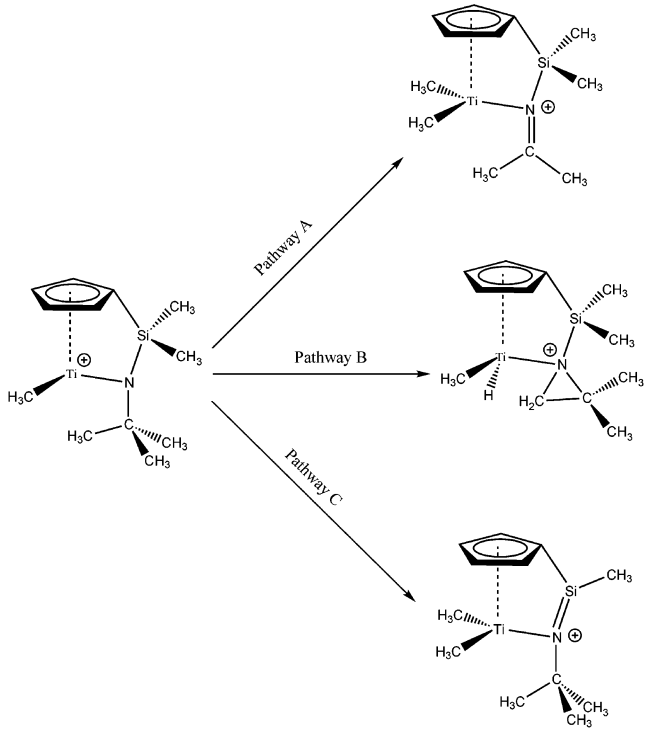

tion. Figure 2 shows optimized geometries of the cation, the transition state, and the corresponding product

Scheme 3. Cationic Decomposition Pathways Involving an Intramolecular C−H Activation

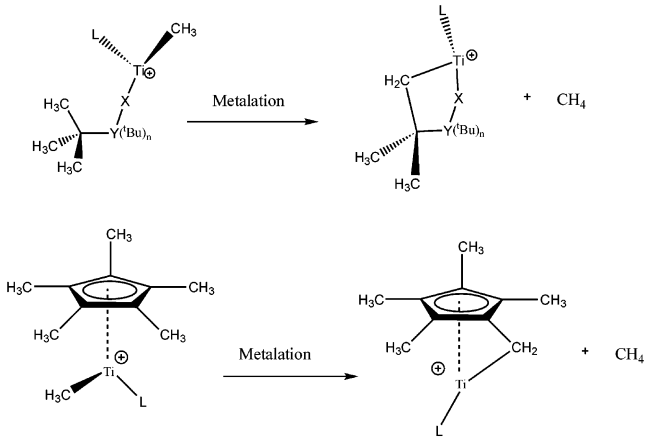

L = Cp, NP^tBu_3

X = N, O; Y = C, Si, P

n = 1, 2

formed from the transfer of methyl on butyl to the central metal for the constrained-geometry catalyst. During the transition state search, as shown in Figure 2, the C−C bond from the *tert*-butyl group was broken and a Ti−C bond was partially formed. A late transition state was predicted for this decomposition pathway.

Table 1 shows the activation energies and the enthalpies of reaction for the transfer of methyl from the ancillary ligand to the cationic metal center (see Scheme 1). As shown in Table 1, the methyl transfer reactions are endothermic and the activation energies fall in the range 16−58.1 kcal/mol. The lowest activation barrier was computed for the constrained-geometry catalyst. The other catalyst systems have higher activation energies and are not likely candidates for this deactivation pathway. This reaction is more facile for the constrained-geometry catalyst, as evidenced by the lowest activation barrier for this system. From Table 1, it is also evident that the methyl transfer reaction for the constrained-geometry catalyst is less endothermic than the other catalyst systems. A bond order analysis was done to characterize the transition states and products formed from the decomposition of the corresponding cations. The key bond orders are shown in Figure 3. As shown in Figure 3a, the formation of a double bond between nitrogen and the carbon of the tertiary butyl group in the product complex explains the higher thermodynamic stability of the constrained-geometry catalyst. The other cationic catalysts considered in this investigation form a three-membered thermodynamic product. As shown in Table 1, the heat of reaction and the activation barriers for these systems are too high for ketimide and phosphinimide systems, and thus, the methyl transfer reaction may not be considered as a possible deactivation pathway for these systems.

We have also considered a different decomposition route for the constrained-geometry catalyst. This involves the transfer of methyl from silicon to the cationic metal center (pathway C, Scheme 2). This is not the case for the other catalyst systems, as they do not contain any methyl group on silicon. The activation barrier and the heat of reaction for this process are 32.3 and 26.4

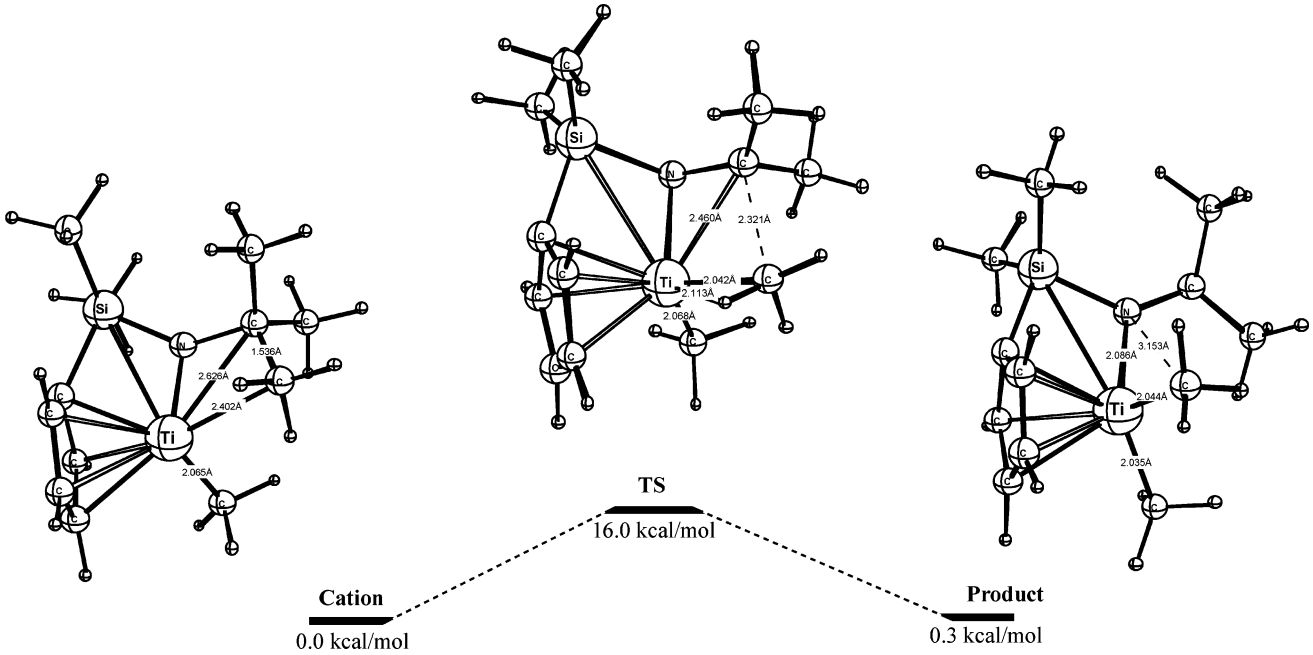

Figure 2. Optimized geometries (Å) of the cation, the transition state, and the product formed from the transfer of methyl on butyl to the metal for the constrained-geometry catalyst.

Table 1. Activation Energies and Heat of Reaction (kcal/mol) for Methyl Transfer from the Ancillary Ligand to the Metal Center

cat.	heat of reaction	activation energy
$(CpSiMe_2N^tBu)TiMe^+$	0.3	16.0
$(Cp)NP^tBu_3TiMe^+$	30.5	58.1
$(NP^tBu_3)_2TiMe^+$	23.2	32.4
$(Cp)(NC^tBu_2)TiMe^+$	19.6	58.4
$(Cp)(OSi^tBu_3)TiMe^+$	35.9	38.2

kcal/mol, respectively. Thus, pathway C is not competitive with pathway A. As shown in Figure 3b, the π-overlap between Si and N is not as strong as the π-overlap between C and N. The Si−N bond order is 1.5, whereas the C−N bond order is 1.8. Therefore, the C−N bond has more of a double-bond character than the Si−N bond. This presumably explains the reason pathway A is thermodynamically more stable than pathway C. It is further clear form Table 1 that pathway B may not be considered as a possible thermal decomposition route for the constrained-geometry catalyst.

Table 2 depicts the activation energies and the heat of reaction for hydrogen transfer from the methyl group on the ancillary ligand to the metal. As shown in Table 2, we have investigated this reaction for all the catalyst systems considered in this study (see Figure 1). The activation barriers fall in the range 43−60 kcal/mol. The activation barriers are too high, and thus, this deactivation pathway is not a likely possible decomposition route for all the catalysts.

As shown in Scheme 1, the transfer of *tert*-butyl from the ancillary ligand to the metal center is also a possible decomposition pathway. However, this is not the case for the constrained-geometry catalyst. Table 3 shows the activation energies and the heat of reaction for ketimide, siloxy, phosphinimide, and bis(phosphinimide) systems. It is evident from Table 3 that the *tert*-butyl transfer reaction is endothermic. The *tert*-butyl transfer reaction is more facile than the corresponding hydrogen and methyl transfer reactions from the ancillary ligand to the metal. It is instructive to compare the thermodynamic stabilities of the products formed from this decomposition pathway. The ketimide system is thermodynamically more stable than the other complexes. This can be understood through a bond order analysis method.

A bond order analysis was carried out in order to characterize the nature of the Ti−C (methyl), Ti−C (Cp), N−P, N−C, and O−Si bonds. The Ti−C (*tert*-butyl) bond was also examined in the product complex. Figure 4 presents key bond orders for the four catalyst systems involving the *tert*-butyl group transfer reaction. It is clear from Figure 4 (a, b, c, and d) that the Ti−C (Cp), Ti−C (methyl), and Ti−P (this is the case for the bis(phosphinimide) system) bond orders do not change significantly. The N−P, N−C, and O−Si bond orders increase substantially during the reaction. However, the Ti−N and Ti−O bond orders decrease significantly in the product complex. Also, we find that the total bond order is approximately conserved during the decomposition reaction.

As shown in Table 3, the bis(phosphinimide) and the phosphinimide systems are thermodynamically less stable than the siloxy and ketimide complexes. Also, the bis(phosphinimide) and phosphimide systems have higher bond orders around titanium than the above complexes. The electron-rich metal center in bis(phosphinimide) and phosphinimide systems cannot accept readily the incoming *tert*-butyl substituent. This is reflected by the highest heat of reaction and activation barriers reported for these systems. The electron-deficient metal center in ketimide and siloxy complexes, on the other hand, can accept readily the incoming *tert*-butyl group from the decomposition reaction. The high thermodynamic stability of the ketimide system is due to the formation of a triple bond between the nitrogen and the sp^2 carbon of the ancillary ligand. The triple-bond character of the C−N bond is shown in Figure 4d. This appears to be

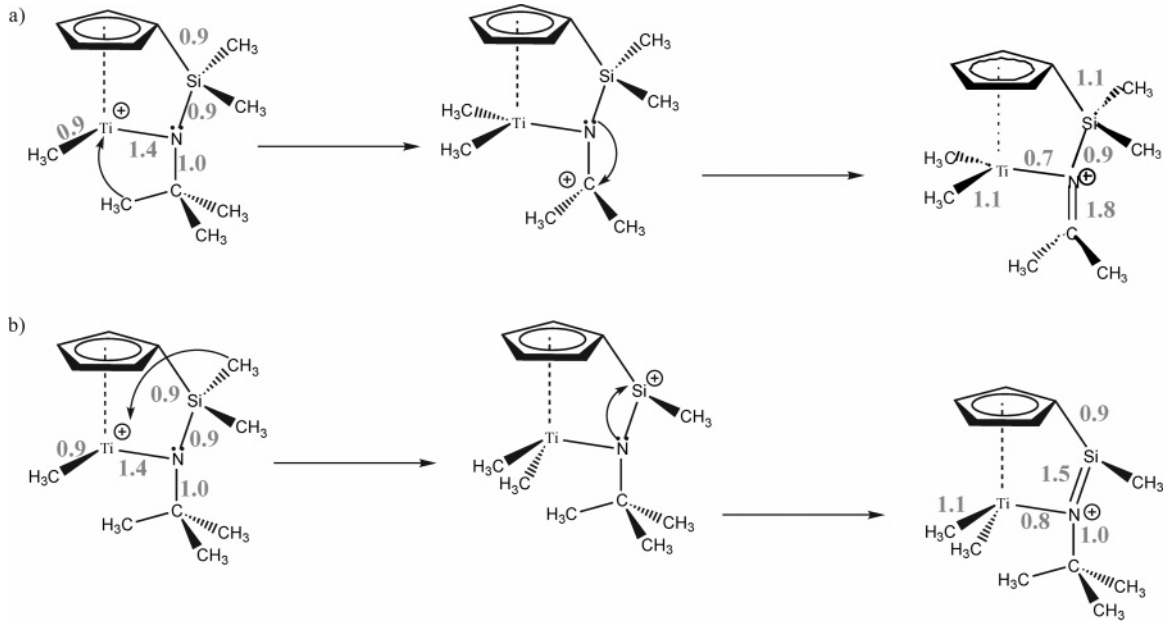

Figure 3. Key bond orders for the transfer of methyl on butyl to the metal center (a) and the transfer of methyl on Si to the metal center (b). The bond order analysis is shown for the constrained-geometry catalyst.

Table 2. Activation Energies and Heat of Reaction (kcal/mol) for Hydrogen Transfer from the Ancillary Ligand to the Metal Center

cat.	heat of reaction	activation energy
$(CpSiMe_2N^tBu)TiMe^+$	26.0	60.0
$(Cp)NP^tBu_3TiMe^+$	30.5	59.8
$(NP^tBu_3)_2TiMe^+$	23.2	62.9
$(Cp)(NC^tBu_2)TiMe^+$	17.9	43.2
$(Cp)(OSi^tBu_3)TiMe^+$	38.9	56.7

Table 3. Activation Energies and Heat of Reaction (kcal/mol) for Butyl Transfer from the Ancillary Ligand to the Metal Center

cat.	heat of reaction	activation energy
$(CpSiMe_2N^tBu)TiMe^+$	*a*	*a*
$(Cp)NP^tBu_3TiMe^+$	26.6	41.2
$(NP^tBu_3)_2TiMe^+$	17.9	29.4
$(Cp)(NC^tBu_2)TiMe^+$	1.8	28.8
$(Cp)(OSi^tBu_3)TiMe^+$	15.0	24.9

[a] This reaction is not operating for the constrained-geometry catalyst.

the key factor that results in the stabilization of the ketimde catalyst systems.

Scheme 3 shows a decomposition pathway involving the transfer of hydrogen from Cp* to the growing polymer. This reaction produces methane and a ring-metalated, metallacyclic complex, as shown in Scheme 3. This is a commonly observed deactivation pathway. Marks et al. have reported reaction of bulky $(1,3\text{-}^tBu_2Cp)_2ZrMe_2$ with $B(C_6F_5)_3$ to produce a C−H activated metallacyclic cation.[20] This reaction is inert with respect to ethylene polymerization or oligomerization. Marks et al. have also observed reaction of Cp^*TiMe_3 and $B(C_6F_5)_3$ to form an intramolecularly metalated fulvene-type cationic complexes and methane.[21] Such complexes have been observed previously in the case of the constrained-geometry catalyst dibenzyl precursors.[22] Erker et al. have also observed facile intramolecular C−H activation at Cp-(dimethylamino)-alkyl substituents by methylzirconocene cation to form cyclometalated zirconocenium products.[23]

Table 4 shows activation energies and heat of reaction for the transfer of hydrogen from Cp* to the growing polymer. To our knowledge, this is the first investigation of a C−H activation/decomposition pathway for the naked cation L_2TiMe^+. As shown in Table 4, these reactions are endothermic and the activation barriers are below 31 kcal/mol. Thus, the transfer of hydrogen from Cp* to the methyl group of L_2TiMe^+ is a potential deactivation pathway. Furthermore, the activation barriers correlate well with the electron-donating ability of the ancillary ligands. The highest activation barrier was reported for the phosphinimide system, in line with the high electron-donating ability of the ligand. The electron-rich titanium center in the phosphinimide system has the lowest tendency to accept the incoming anionic carbene from the Cp*. On the other hand, the electron-deficient systems have the highest tendency to accept the carbene from the cyclopentadienyl ring. Therefore, electron-donating ligands and sterically demanding substituents play a crucial role in elevating the activation barrier.

Table 5 depicts the heat of reaction and the activation energies for the transfer of hydrogen from the ligand to the methyl group of L_2TiMe^+. As discussed above, this reaction produces methane and a metalacyclic complex. From a thermodynamic as well as a kinetic point of view, this reaction is the most facile decomposition pathway. A key question is, why is this deactivation pathway more facile than the other metalation reaction? The explanation lies in the electron-donating abilities of C_5H_5 and C_5Me_5 ligands. For C_5Me_5-ligated systems, the metal center is electron-rich, and thus the interac-

(20) (a) Yang, X.; Stern, C. L.; Marks, T. J. *J. Am. Chem. Soc.* **1994**, *116*, 10015. (b) Yang, X.; Stern, C. L.; Marks, T. J. *J. Am. Chem. Soc.* **1991**, *113*, 3623.

(21) Chen, Y.-X.; Metz, M. V.; Li, L.; Stern, C. L.; Marks, T. J. *J. Am. Chem. Soc.* **1998**, *120*, 6287.

(22) Chen, Y.-X.; Marks, T. J. *Organometallics* **1997**, *16*, 3649.

(23) Bertuleit, A.; Fritze, C.; Erker, G.; Frohlich, R. *Organometallics* **1997**, *16*, 2.

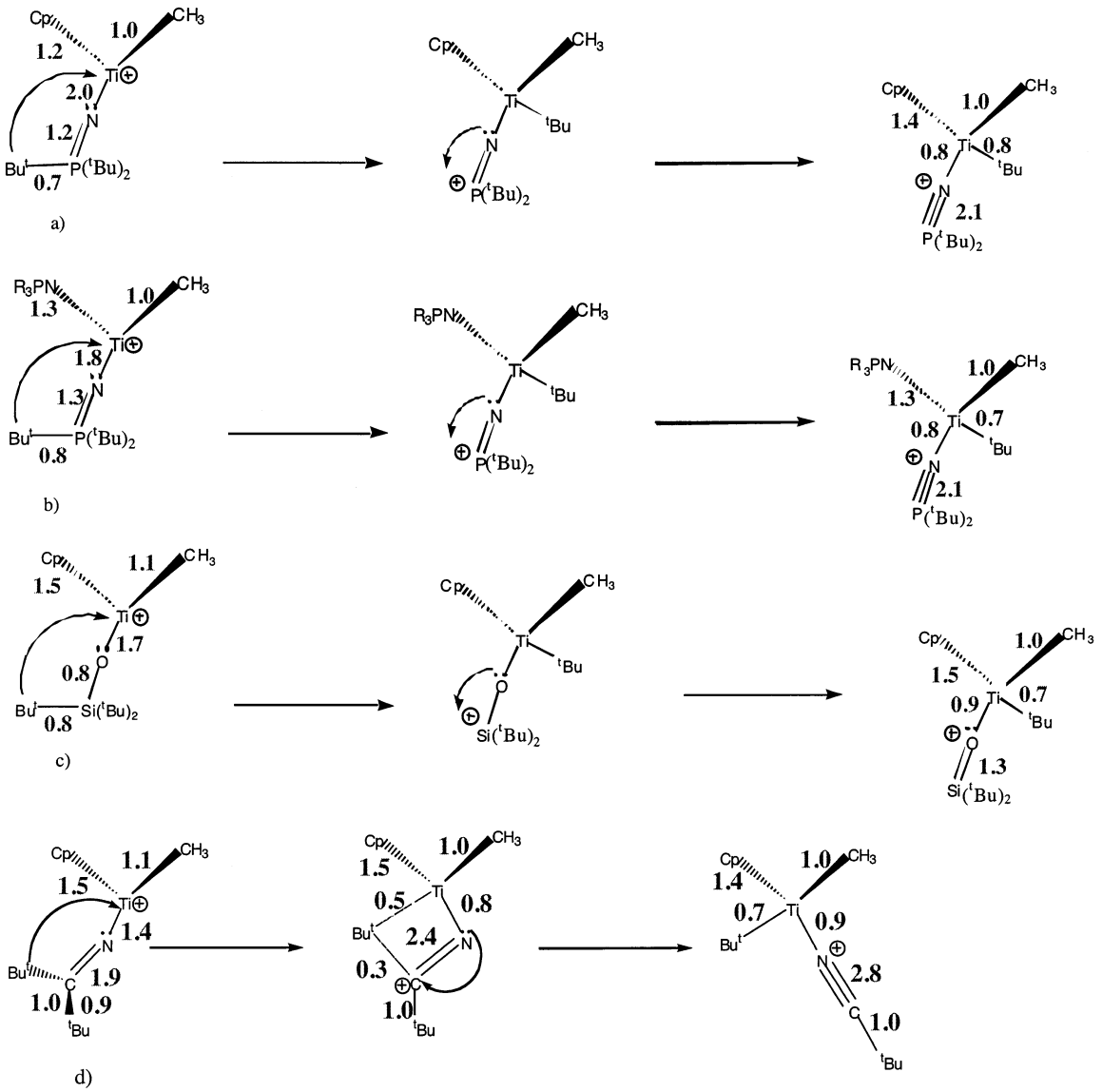

Figure 4. Key bond orders for the transfer of *tert*-butyl from the ancillary ligand to the metal center. The bond order scheme involves phosphinimide (a), bis(phopshinimide) (b), siloxy (c), and ketimide (d) catalyst systems.

Table 4. Activation Energies and Heat of Reaction (kcal/mol) for Hydrogen Transfer from Cp* to the Growing Polymer

cat.	heat of reaction	activation energy
$(CpSiMe_2N^tBu)TiMe^+$	19.9	30.4
$(Cp)NP^tBu_3TiMe^+$	12.2	31.4
$(NP^tBu_3)_2TiMe^+$	*a*	*a*
$(Cp)(NC^tBu_2)TiMe^+$	18.6	28.6
$(Cp)(OSi^tBu_3)TiMe^+$	15.0	26.7

[a] This is not applicable for the bis(phosphinimide) catalyst.

Table 5. Activation Energies and Heat of Reaction (kcal/mol) for Hydrogen Transfer from the Ancillary Ligand to the Growing Polymer

cat.	heat of reaction	activation energy
$(CpSiMe_2N^tBu)TiMe^+$	16.5	17.5
$(Cp)NP^tBu_3TiMe^+$	9.8	21.2
$(NP^tBu_3)_2TiMe^+$	9.4	22.6
$(Cp)(NC^tBu_2)TiMe^+$	16.9	20.7
$(Cp)(OSi^tBu_3)TiMe^+$	2.6	19.2

tion between the metal and the CH_2 carbon is weak. This is reflected by the high barriers reported for the transfer of hydrogen from the Cp* ring to the methyl group of L_2TiMe^+ (see Table 4). For C_5H_5-ligated systems, the metal center is electron-deficient. The interaction between the metal and the CH_2 carbon is relatively strong. This is also reflected by the lowest barriers reported for this decomposition pathway.

Conclusions

In summary, we have presented a quantum chemical study of deactivation pathways involving the cationic catalyst L_2TiMe^+. For weakly coordinating anions, the catalytic active species can be regarded as an essentially free cation, especially in polar solvents. Thus, the calculations have been carried out on the free cationic catalyst system L_2TiMe^+, which is an acceptable model for a weakly bound anion (e.g., $[B(C_6F_5)_4]^-$). The transfer of butyl from the ancillary liagnd to the metal is a likely decomposition pathway for ketimide, siloxy, phosphinimide, and bis(phosphinimide) systems. The transfer of methyl from the ancillary liagnd to the metal is not a possible decomposition pathway for ketimide and phosphinimide systems. For the constrained geometry catalyst, the transfer of methyl from the ligand to the metal

is a potential decomposition pathway. The transfer of methyl from Si to the metal center is also a likely decomposition pathway for the constrained-geometry catalyst. Furthermore, the transfer of hydrogen from the ancillary ligand to the cationic metal center is not a likely decomposition pathway for ketimide, siloxy, phophinimide, bis(phosphinimide), and the constrained-geometry catalyst systems.

We have also studied two potential deactivation pathways that involve hydrogen transfer from the ancillary ligand to the methyl group of L_2TiMe^+. These reactions form methane and a ring-metalated metalacyclic complex. Electron-donating ligands and sterically demanding substituents play a crucial role in elevating the activation barrier.

Acknowledgment. This work was supported by the Natural Science and Engineering Research Council of Canada (NSERC) and by NOVA Research and Technology Corporation (NRTC).

Supporting Information Available: Optimized Cartesian coordinates (Å) for the different catalyst systems. This material is available free of charge via the Internet at http://pubs.acs.org.

OM049478S